Higher seismic performance of GRS integral bridge by cement-mixing the approach fill

Fumio Tatsuoka*
Tokyo University of Science, Japan (tatsuoka@rs.noda.tus.ac.jp)
Ryoichi Soma
Toyo Engineering Corp., Japan
Hiroki Nishikiori
Ibaraki Prefecture, Japan
Kenji Watanabe
Railway Technical Research Institute, Japan
Daiki Hirakawa
Chuo University, Japan

ABSTRACT: A new cost-effective high-performance bridge system, called the GRS integral bridge, was developed alleviating several serious problems with conventional simple girder bridges, including a low seismic stability, massive abutments, a strong need for a pile foundation, bumps immediately behind the abutments and costly construction and long-term maintenance of girder bearings. A pair of geosynthetic-reinforced (GR) approach blocks comprising well-compacted lightly cement-mixed well-graded gravelly soil are constructed to minimize bumps by long-term and seismic settlements relative to the facings and to increase the seismic stability. For a gradual transition from the rigid approach block to relatively soft unreinforced unbound fill behind to minimize bumps and for higher resistance against lateral push-in loads by the inertial of the girder and facing during earthquakes, the approach blocks are trapezoidal with the base wider than the crest. To validate this design concept, a series of shaking table tests were performed on model of 1/10 in scale of prototype.

Keywords: cement-mixed soil, GRS integral bridge, seismic stability, shaking table model tests

1 INTRODUCTION

Conventional simple supported bridges have several inherent drawbacks, including a low seismic stability of approach fills; massive abutments as cantilever structures, a strong need for a pile foundation in usual cases; the development of bumps in the approach fills immediately behind the abutments gradually during long-term service and suddenly by seismic loads; and costly construction and long-term maintenance of the girder bearings. The authors and their colleagues developed a new cost-effective and high-performance bridge system, called the GRS integral bridge, that alleviates these serious problems (Fig. 1; Tatsuoka et a., 2009, 2014, 2016; Munoz et al., 2012; Koda et al., 2013, 2018; Yonezawa et al., 2014; Soga et al., 2018). Now, the GRS integral bridge is one of the standard bridge systems for railways, including high-speed railways (HSRs, Shinkansen in Japanese). Fig. 2 shows the one that was completed recently for a HSR (Kyushu Shinkansen Nagasaki route, Soga et al., 2018).

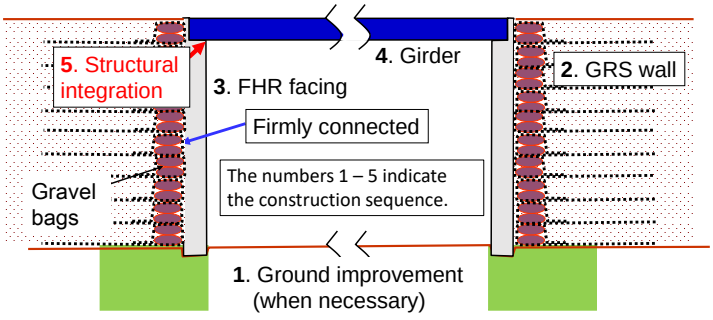

Figure 1. Structure of GRS integral bridge (the numbers denote construction sequence).

a)

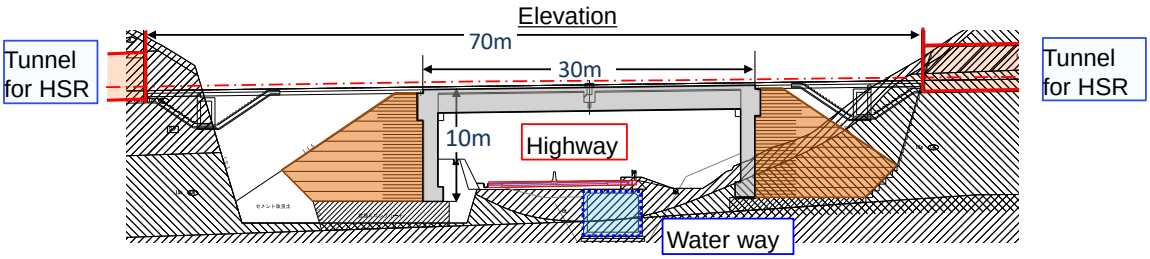

b)

Figure 2. GRS integral bridge at Genshu for HSR (Kyushu Shinkansen, Nagasaki route): a) structure; and b) completed bridge (Soga et al., 2018)

A GRS integral bridge is constructed as shown in Fig. 1. That is, a pair of geosynthetic-reinforced (GR) approach blocks then ordinary unbound fills behind are first constructed. As shown in Fig. 2a, to minimize the long-term and seismic settlements relative to the facings and to increase the seismic stability, the approach blocks comprise well-compacted lightly cement-mixed well-graded gravelly soil that are reinforced with geogrid layers firmly connected to the back of the full-height rigid (FHR) facing that are constructed afterwards. In a particular case shown in Fig. 2, the heel zone of the approach block on the left side is truncated so that the shape becomes the same as the approach block on the right side that lacks a heel zone due to construction on rock foundation so that the response of the bridge system against the thermal deformation of the girder becomes symmetric. As shown in Fig. 3, with ordinary geosynthetic-reinforced soil retaining walls having staged-constructed FHR facings, the geogrid layers are relatively short at lower levels to reduce the amount of excavation when constructed on an existing slope while several geogrid layers at higher levels are made longer to increase the resistance against over-turning failure about the bottom of facing as well as the lateral sliding failure along the bottom of the reinforced zone. With GRS integral bridges, on the other hand, for gradual transition from a rigid approach block of cement-mixed soil to relatively soft unreinforced unbound fills behind to minimize bumps and for higher resistance of the approach block against lateral push-in loads by inertia of the girder and facing during earthquakes, the approach block is trapezoidal with the base wider than the crest. After the deformation of the supporting ground due to the weight of approach blocks and ordinary fills behind has taken place sufficiently, RC FHR facings are constructed integrated to the approach block. Finally, a continuous girder is constructed with both ends integrated to the top ends of the FHR facings. To validate this design concept, a series of shaking table tests on models of 1/10 in scale of prototype were performed.

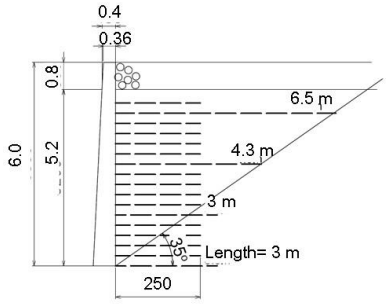

Figure 3. Typical GRS retaining wall with a staged-constructed FHR facing.

2 MODELS AND SHAKING TABLE TEST METHOD

Based on results of a series of model shaking table tests, Tatsuoka et al. (2009) showed that, when the approach block is compacted unbound soil, the most likely mechanism of collapse by severe seismic loads of GRS integral bridge is as follows:

1) The top part of the approach fill yields in the passive mode due to lateral push-in loads caused by horizontal inertia of the girder and facing.
2) The FHR facing starts rotating associated with the yielding of the approach fill developing from the top toward the bottom.
3) The connection between the girder and the FHR facing yields, which accelerates the connection failure between the geogrid and the facing or the rupture of the geogrid or the pull-out failure of geogrid, whichever having the smallest resistance. These events then increase the rotation of the facing about the top.

The resistance of the bridge system against this mode of collapse increases with an increase in the passive earth pressure that can be developed by the approach fills and this resistance can be effectively increased by making the approach blocks sufficiently stable by constructing using well-compacting lightly cement-mixed well-graded gravelly soil. To examine this design concept, the dynamic stabilities of the following three models illustrated in Fig. 4 when subjected to strong horizontal input acceleration were compared:

Model N: The supporting ground and the backfill were made by pluviating in air air-dried Toyoura sand to a relative density D_r equal to 90 %. The water content is about 1% with negligible apparent cohesion. The details of this model were reported by Tatsuoka et al. (2009).

Model R: A pair of rectangular approach blocks were made compacting lightly cement-mixed silica sand, while the supporting ground and the fills behind the approach fills were made using air-dried Toyoura sand in the same way as Model N.

Model T: A pair of trapezoidal approach blocks were made compacting lightly cement-mixed silica sand, while the supporting ground and the fills behind the approach blocks were made using air-dried Toyoura sand in the same way as Model R.

A length similitude ratio, λ, equal to 1/10 was assumed. The models were produced inside a plane strain sand box (2,058 mm-long; 600 mm-wide; 1,400 mm-high). The details of these models are described below.

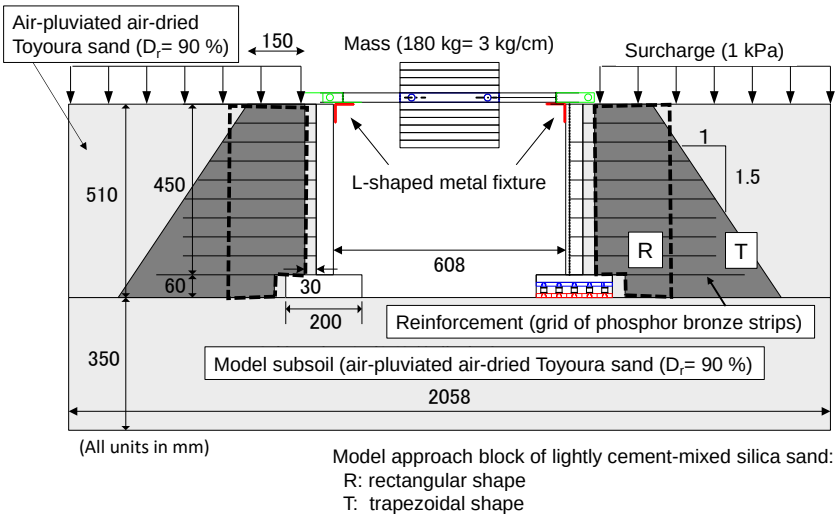

Figure 4 Three models for shaking table tests (N: without cement-mixed sand approach block; R: with rectangular cement-mixed sand approach blocks; and T: with cement-mixed sand trapezoidal approach blocks).

A poorly graded sub-angular sand, Silica No.6 (D_{50}= 0.29 mm; U_c= 0.32/0.13= 2.5; and $(\rho_d)_{max}$= 1.73 g/cm^3 & w_{opt}= 15.6 % by Standard Proctor) was used to produce the model approach blocks, which are rectangular (200 mm-wide, 510 mm high and 600 mm-thick) with model R; and trapezoidal (150 mm-wide (crest); 490 mm-wide (bottom); 510 mm high; and 600 mm-thick) with model T. The cement-mixed sand with a mixing cement/sand mass ratio, c/s, of 4 % was compacted so that the unconfined compressive strength, q_u, became about 200 kPa, which satisfies a similitude ratio λ=1/10 for q_u= 2 MPa assumed for the prototype. The molding water content was set to be relatively high, equal to "w_{opt}=15.6 %" +

2 %= 17.6 %, so that sand and cement is uniformly mixed. The stiffness of the cement-mixed sand zone immediately before the start of shaking was evaluated by means of a miniature falling weight deflectmeter and found to be larger by a factor of about 6 than the unbound Toyoura sand zone. To observe the deformation of the backfill by shaking, thin horizontal layers of black-dyed sand were placed at a vertical spacing of 10 cm immediately behind the front transparent side wall (Fig. 5a). On the crest of the backfill, a surcharge of 1 kPa made of lead shots was placed to simulate the weight of road base for railways. The reinforcement was a grid made of phosphor bronze consisting of 17 longitudinal strands with a tensile rupture strength equal to 359 N per strand (Fig. 5b). This strong model grid was selected to measure tensile forces by using electric-resistance strain gauges while assuming that a geogrid that does not exhibit tensile rupture is not used for prototype GRS integral bridges. The covering ratio of the geogrid was 10.1 %. The surface of the strands was made rough, with a friction angle equal to 35 degrees at confining pressure equal to 50 kPa, by gluing sand particles. The respective reinforcement layers were fixed to the back of the facing by using six bolts for a width of 590 mm. In Fig. 5a, the reinforcement layers are indicated by horizontal broken lines.

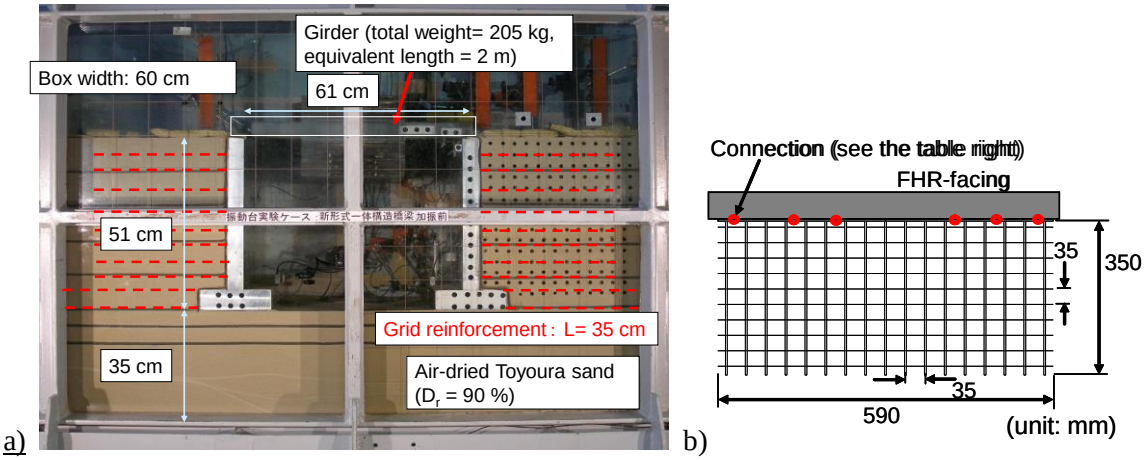

Figure 5 Model N (w/o cement-mixed sand zone); a) side view; and b) model reinforcement

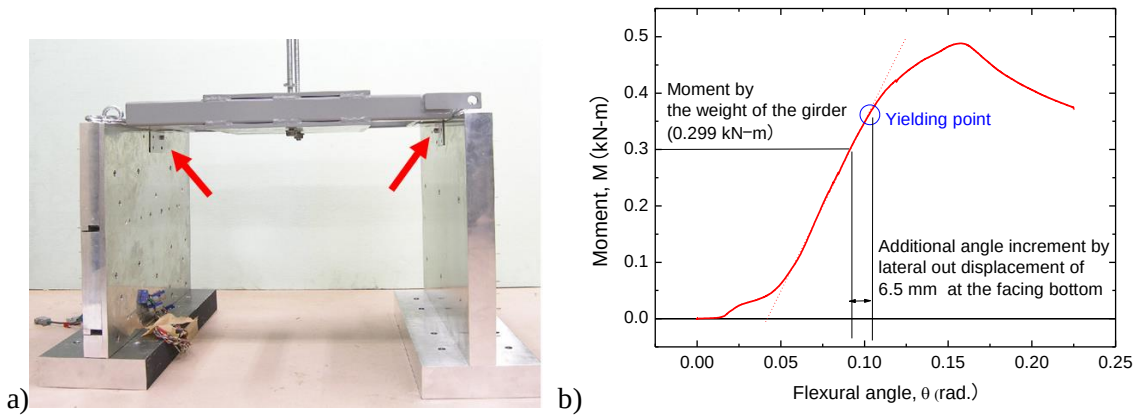

Figure 6. a) Model girder and facings integrated by using a pair of L-shaped metal fixtures (indicated by arrows); and b) bending properties of the fixtures (the angle positive for closing: 0.1 radian= 5.73 degrees).

With the three bridge models N, R and T, the model FHR facing was 51 cm-high and the girder was 61 cm-long. The facings were made of duralumin, all having a bottom width equal to 20 cm. The back and bottom faces of the facings were made rough by gluing sand paper (#150). A mass of 180 kg was attached to the center of the model girder, which made the total weight of the girder equal to 205 kg for an equivalent length equal to 2 m (i.e., 20 m in the assumed prototype). No pile foundation supporting the facings was used to evaluate the dynamic stability in the most likely collapse mode of usual prototype GRS integral bridges not using pile foundations. The girder and facings were connected to each other by using a L-shaped metal fixture (Fig. 6a). The fixtures were 3 mm-thick, 50 mm-wide and 200 mm-long. The fixture starts yielding at a flexural angle equal to about 0. 1 radian (i.e., about 6 degrees, equivalent to about 10 % shear strain in the backfill, Fig. 6b). The peak resisting moment, about 0.5 kN-m, is much smaller, by a factor of about 1/3, than the value necessary to resist against the moment produced by the earth pressure activated on the back of the facing of model N.

Twenty sinusoidal waves at a frequency, f_i, of 5 Hz were applied at the shaking table step by step increasing the amplitude of horizontal acceleration, α_b, by an increment of 100 gal. This input frequency is much smaller than the initial predominant frequency, f_0, of these models, equal to about 30 Hz and a ratio of f_i to f_0 equal to 6 is similar to the one of ordinary prototype GRS integral bridges (Munoz et al., 2012). Time histories of the following physical quantities were measured during shaking: i.e., lateral displacement at the facing top; settlement of the crest of approach fills at distances equal to 5 cm and 35 cm from the back of the facing; the rotational angle of the facing; and local earth pressures and shear stresses at the back of the facing with nine local two-component load cells with one at the heel of the facing footing. As the total area of the sensing faces of these local load cells is the same as the area of the whole back face of the facing, the distributions of earth pressure and shear stress can be obtained directly from their outputs (as shown later).

3 TEST RESULTS

3.1 *Performance when using rectangular approach blocks*

Fig. 7a shows the residual deformation of models N and R plotted against the amplitude of table horizontal acceleration, α_b, at the immediately preceding shaking stage. Both models exhibit essentially no residual deformation before α_b becomes about 800 gal. As α_b increases more, the settlement at 5 cm back of the facing on the crest of the approach fill starts increasing correspondingly to the rotational displacement of the facing, which increases at a rate that increases with an increase in α_b. After α_b becomes larger than about 800 gal, the value of α_b at the same residual rotational angle of the facing is larger by about 100 gal with model R than with model N. This result indicates that the rectangular cement-mixed sand zones increased the dynamic stability of the bridge system. Fig. 7b shows the time histories of the rotational angle of the facing at shaking stages where α_b is about 1,050 gals of models N and R. At this stage, the top part of the approach fill of model N is yielding in the passive model significantly due to increasing push-in lateral loads. With model R, on the other hand, the rotational angle of the facing is not yet increasing significant, showing that the passive yielding of the approach blocks and unbound fills behind is not yet significant.

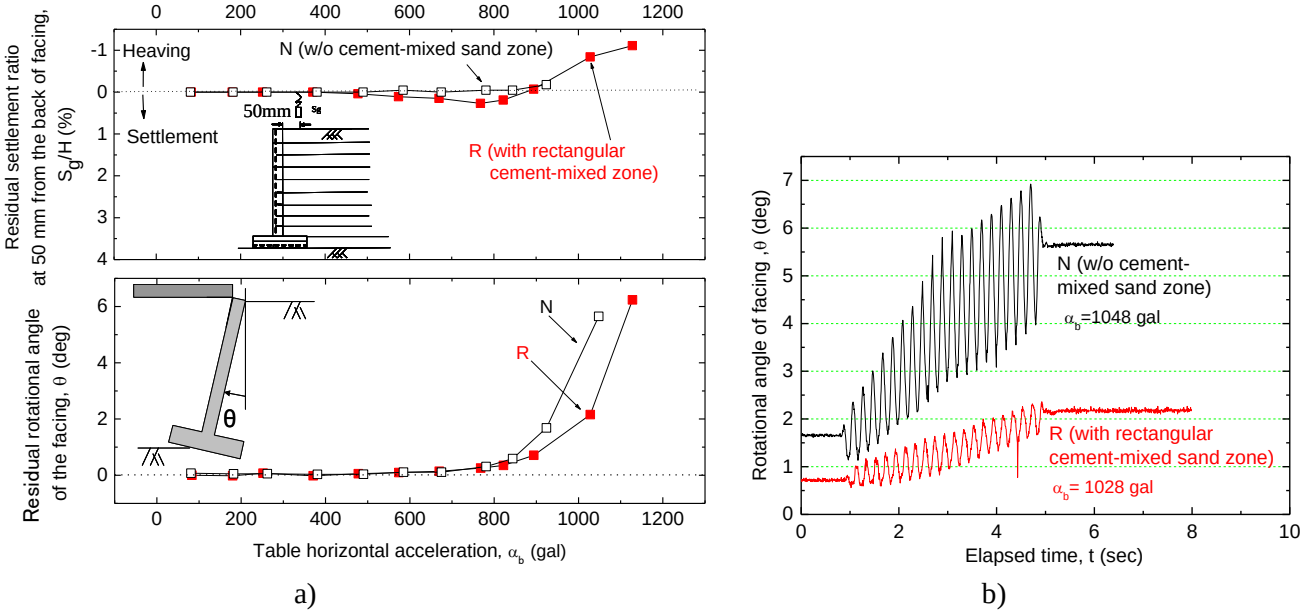

Figure 7. Deformation of models N and R: a) residual deformation vs. input horizontal acceleration; and b) typical time histories of the rotational angel of facing during shaking.

Fig. 8 shows the distributions of the passive earth pressure on the back of the facing at different shaking stages (i.e., the largest value of the maximum earth pressure in each loading cycle at each shaking state) of models N and R. With model N, after the approach fill starts yielding when α_b becomes about 800 gal, the passive pressure stops increasing rather proportionally to an increase in α_b. On the other hand, with

model R, after α_b becomes about 800 gal and until α_b becomes about 1,000 gal, the passive pressure on the top half of the facing keeps increasing rather proportionally to an increase in α_b, showing that the approach blocks effectively resist the lateral push-in loads despite that yielding is taking place to some extent. However, as α_b becomes larger than about 1,000 gal, the passive pressure on the top half of the facing suddenly decreases while the passive pressure around the middle height of the facing increases significantly, indicating significant yielding of the top part of the approach blocks. As no obvious evidence of significant failure was observed in the approach blocks of cement-mixed sand of the model R when dismantled after the end of shaking, it seems that the top part of the unbound Toyoura sand fill immediately back of the approach block yielded significantly in the passive mode. In Fig. 9, the sketches of models N and R after the end of shaking are shown. It may be seen that the distance between the footings of the facings on both sides of models N and R has decreased largely, in particular with model N. These results indicate that it is effective for an increase of the seismic stability of GRS integral bridge to introduce approach block comprising cement-mixed soil, whereas it is not very effective if the cement-mixed soil zone is rectangular with a relatively small width.

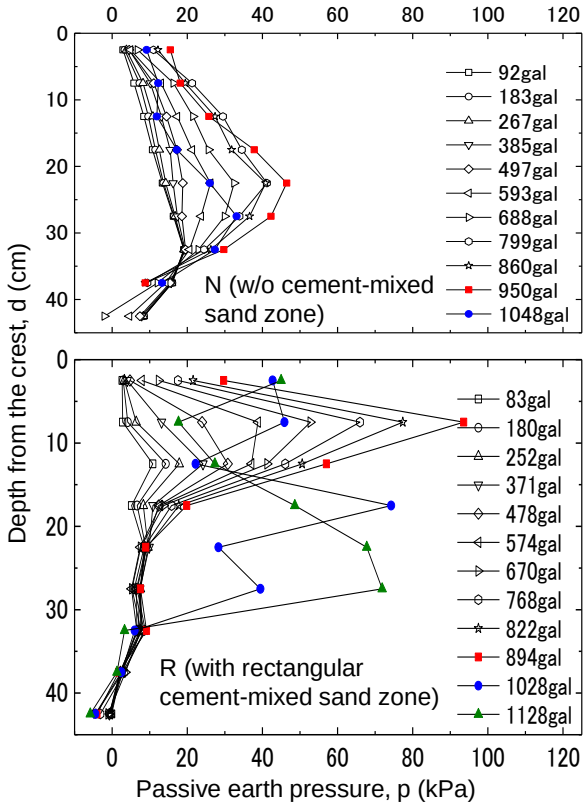

Figure 8 (left). Distributions of passive earth pressure on the back of the facing at different shaking stages of models N and R.

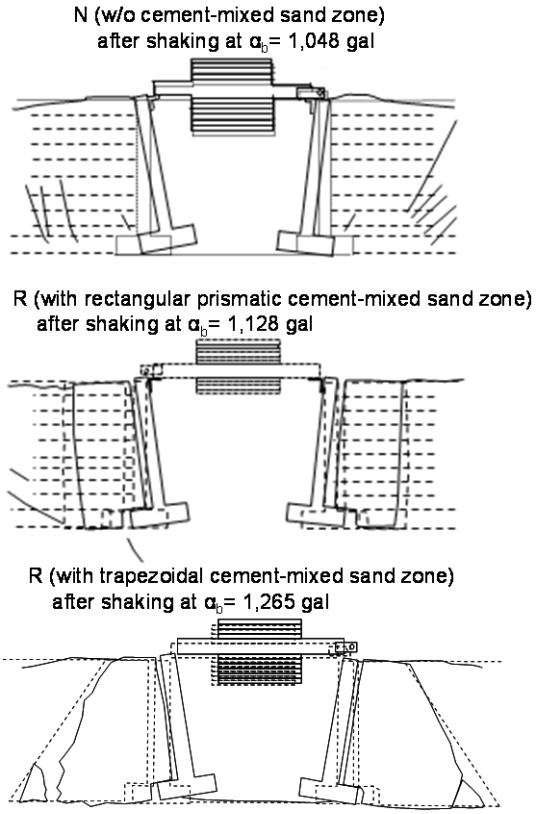

Figure 9 (right). Sketches of models N, R and T after the end of shaking.

3.2 *Performance when using trapezoidal approach blocks*

Fig. 10a shows the residual settlements at 5 cm and 35 cm from the back of the facing and the rotational angle of the facing plotted against the amplitude of horizontal acceleration at the table of models N and T. The crest of the approach fill of model N does not exhibit settlement but heaves due to the passive failure of the unbound Toyoura sand fill. The heaving at the crest of the cement-mixed zone of model T is due to the rotational displacement of the approach block of cement-mixed sand and the facing together (Fig. 10b). It may be seen from Fig. 10b that, after α_b becomes larger than about 900 gal, the value of α_b at the same residual rotational angle of the facing is larger by about 200 gal with model T than with model N (i.e., larger by about 100 gal with model T than with model R). This result indicates that the trapezoidal cement-mixed sand zones of model T increases the seismic stability of the bridge to a larger extent than the rectangular cement-mixed sand zoness of model R.

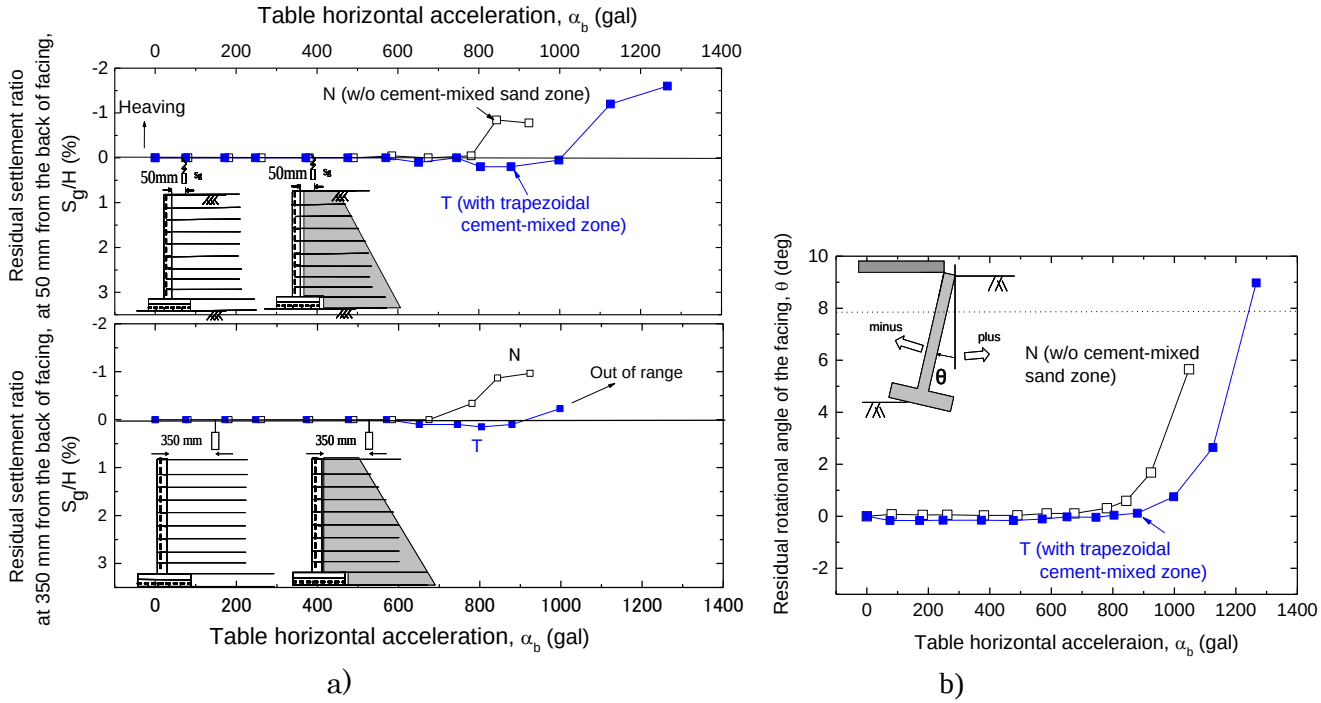

Figure 10. Deformation of models N and T: a) residual settlement and b) rotational angle of facing vs. input horizontal acceleration.

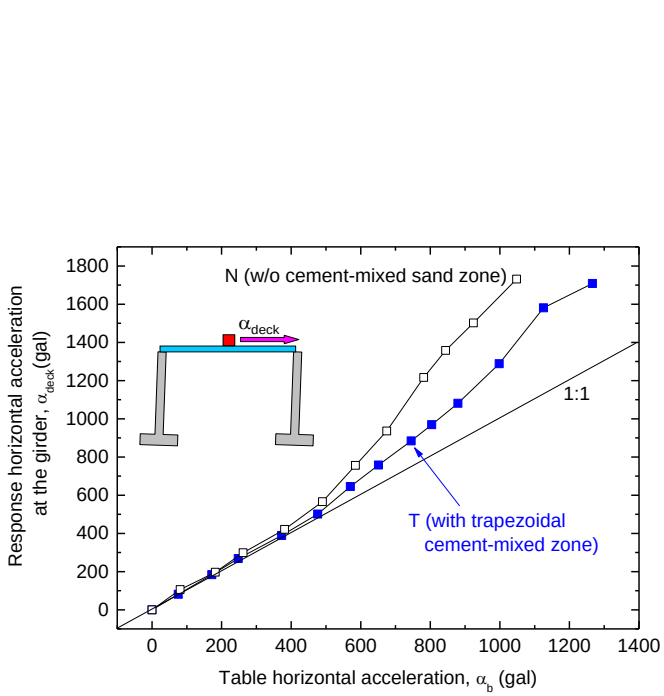

Figure 11 (left). Relationship between the input acceleration at the table and the response acceleration at the girder of models N and T.

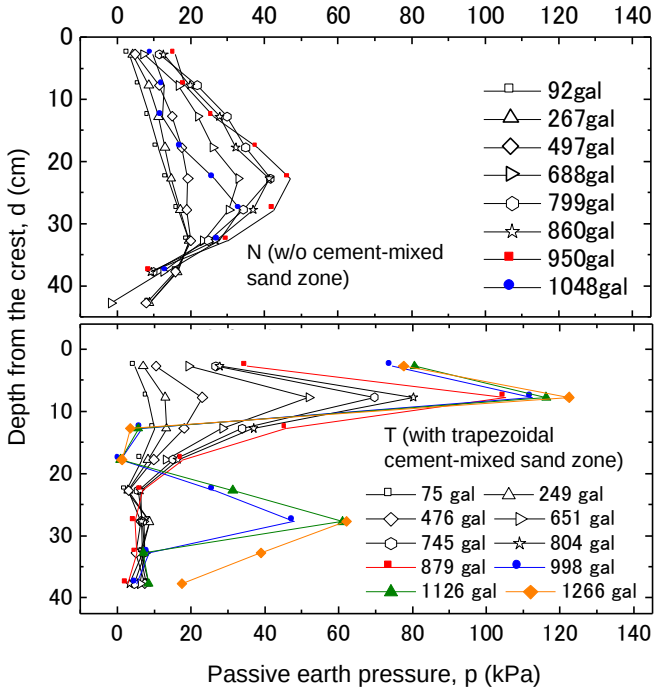

Figure 12 (right). Distributions of passive earth pressure on the back of the facing at different shaking stages of models N and T.

Fig. 11 shows the relationship between the input acceleration at the table, α_b, and the response acceleration at the girder, α_{deck}, in the course of the shaking table tests of models N and T. The amplification ratio defined as α_{deck}/α_b increases at a smaller rate with model T than model N, showing that the trapezoidal approach blocks of cement-mixed sand increases the dynamic stability of the bridge. Fig. 12 shows the distributions of passive earth pressure on the back of the facing at different shaking stages of models N and T. With model T, the top part of the trapezoidal approach block resists effectively lateral push-in loads until the end of test, unlike the rectangular approach blocks of model R (Fig. 8). After α_b becomes larger about 1,000 gal, the passive earth pressure at the top part of the approach blocks stops increasing, while the passive pressure just above the bottom of the facing of model T starts increasing. This trend in-

dicates yielding of the top part of the approach blocks to some extent associated with more significant passive failure in the unbound Toyoura sand zone immediately behind. It was observed that the heel zone in the trapezoidal approach blocks of model T started cracking when α_b was about 1,000 gal and this became obvious at the end of the test, as shown in Fig. 9. It was found that vertical cracks developed at the end of reinforcement layers in the approach blocks (see Fig. 4).

4 CONCLUSIONS

The seismic stability of GRS integral bridge increases by introducing a cement-mixed soil zone, called an approach block, immediately back of each facing in the approach fill. This measures becomes more effective by: a) increasing the monolithic stability of the cement-mixed soil zone by adopting a trapezoidal shape with a sufficient base width that is wider than the crest; b) making the shear strength of cement-mixed soil sufficiently high (if possible by using well-compacted cement-mixed well-graded gravelly soil); and c) arranging geogrid layers in the whole of the approach block of cement-mixed soil zone. The current design of GRS integral bridges follows these design concepts, as typically seen from Fig. 2a.

REFERENCES

Koda, M., Nonaka, T., Suga, M., Kuriyama, R., Tatetama, M. and Tatsuoka, F. 2013. A series of lateral loading tests on a full-scale model of Geosynthetic- Reinforced Soil Integral Bridge, *Proc. International Symposium on Design and Practice of Geosynthetic-Reinforced Soil Structures*.

Koda, M., Nonaka, T., Suga. M., Kuriyama, R., Tateyama, M. and Tatsuoka, F. 2018. Lateral cyclic loading tests of a full-scale GRS integral bridge model, *Proc. 11ICG*, Seoul.

Munoz, H., Tatsuoka, F., Hirakawa, D., Nishikiori, H., Soma, R., Tateyama, M. and Watanabe, K. 2012. Dynamic stability of geosynthetic-reinforced soil integral bridge, *Gesynthtetics International*, Vol.19, No.1, pp.11-38.

Soga, D., Takano, Y., Yonezawa, T., Koda, H., Tatsyma, M. and Tatsuoka, F. 2018. Design and construction of various type GRS structures for a new high-speed railway, Proc. 11ICG, Seoul.

Tatsuoka, F., Hirakawa, D., Nojiri, M., Aizawa, H., Nishikiori, H., Soma, R., Tateyama, M. and Watanabe, K. 2009. A new type integral bridge comprising geosynthetic-reinforced soil walls, *Gesynthtetics International*, IS Kyushu 2007 Special Issue, Vol.16, No.4, pp.301-326.

Tatsuoka, F., Tateyama, M., Koseki, J. and Yonezawa, T. 2014. Geosynthetic-Reinforced Soil Structures for Railways in Japan, *Transportation Infrastructure Geotechnology*, Springer, Vol.1, No.1, pp.3-53.

Tatsuoka, F., Tateyama, M., Koda, M., Kojima, K., Yonezawa, T., Shindo, Y. and Tamai, S. 2016. Research and construction of geosynthetic-reinforced soil integral bridges, *Transportation Geotechnics*, Vol.8, pp.4-25.

Yonezawa, T., Yamazaki, T., Tateyama, M. and Tatsuoka, F. 2014. Design and construction of geosynthetic-reinforced soil structures for Hokkaido high-speed train line, *Transportation Geotechnics*, Vol.1, No.1, pp.3-20.